FERMILAB-CONF-17-318-TD
ACCEPTED

Summary of Test Results of MQXFS1 - the First Short Model 150 mm Aperture Nb_3Sn Quadrupole for the High-Luminosity LHC Upgrade

S. Stoynev, G. Ambrosio, M. Anerella, R. Bossert, E. Cavanna, D. Cheng, D. Dietderich, J. DiMarco, H. Felice, P. Ferracin, G. Chlachidze, A. Ghosh, P. Grosclaude, M. Guinchard, A. R. Hafalia, E. Holik, S. Izquierdo Bermudez, S. Krave, M. Marchevsky, F. Nobrega, D. Orris, H. Pan, J. C. Perez, S. Prestemon, E. Ravaioli, G. Sabbi, T. Salmi, J. Schmalzle, T. Strauss, C. Sylvester, M. Tartaglia, E. Todesco, G. Vallone, G. Velev, P. Wanderer, X. Wang, M. Yu

***Abstract*—The development of Nb_3Sn quadrupole magnets for the High-Luminosity LHC upgrade is a joint venture between the US LHC Accelerator Research Program (LARP)* and CERN with the goal of fabricating large aperture quadrupoles for the LHC interaction regions (IR). The inner triplet (low-β) NbTi quadrupoles in the IR will be replaced by the stronger Nb_3Sn magnets boosting the LHC program of having 10-fold increase in integrated luminosity after the foreseen upgrades. Previously LARP conducted successful tests of short and long models with up to 120 mm aperture. The first short 150 mm aperture quadrupole model MQXFS1 was assembled with coils fabricated by both CERN and LARP. The magnet demonstrated strong performance at the Fermilab's vertical magnet test facility reaching the LHC operating limits. This paper reports the latest results from MQXFS1 tests with changed pre-stress levels. The overall magnet performance, including quench training and memory, ramp rate and temperature dependence, is also summarized.**

*** The US contributions to the HL-LHC upgrade will be under the US HL-LHC Accelerator Upgrade Project (US HL-LHC AUP)**

***Index Terms*—High Luminosity Large Hadron Collider (LHC), interaction regions, low-β quadrupoles, Nb_3Sn magnets**

I. Introduction

ONE of the main goals of the approved LHC upgrade, HL-LHC, is to allow significant increase of the integrated luminosity, 10-fold, over a period of 10 years. To achieve it a corresponding 5-fold increase of the instantaneous luminosity is planned based in part on replacing focusing magnets with shorter and stronger ones [1]. Thus, requirements set for the HL-LHC include the fabrication of Inner Triplet quadrupole magnets with aperture of 150 mm and nominal operating field gradient of 132.6 T/m [2]. To develop those magnets CERN and LARP joined efforts, fabricating and evaluating short, 1.2 m magnetic length models. Prototypes with 4.2 m magnetic length are being pursued by LARP as a next step [3].

The first short model of this type, MQXFS1a, was tested at the Fermilab's Vertical Magnet Test Facility in early 2016 and reached the operational (16470 A) and ultimate (17890 A) currents [4]. Nevertheless, potentially damaging for the coil(s) "un-loading" led to shortening of the test program and consequent increase of magnet pre-stress levels. After the first test cycle the azimuthal pre-stress was increased by 25% (to 100 MPa on the pole) [5] and the magnet retested as MQXFS1b. A third test cycle, MQXFS1c, was performed where the longitudinal pre-stress was also increased by 65% (to 1 MN force on the rods) [5]. This paper reports new performance results from the three tests cycles and summarizes the performance of the MQXFS1 magnet.

II. MAGNET DESIGN AND INSTRUMENTATION

MQXFS1 is a cos-2θ design model with large 150 mm aperture and short coils. Two of the coils were fabricated by BNL, FNAL and LBNL as part of LARP (coil 3 and 5) and the remaining two by CERN (coils 103 and 104). LARP and CERN coils used RRP 108/127 and RRP132/169 strand architectures, respectively. The magnet structure was encompassed by aluminum shells and aluminum rods were connected to end plates defining the pre- stress levels of the quadrupole. More detailed description of the design and parameters of MQXFS1 can be found in [4], [6], [7].

For convenience, Short Sample Limits (SSL) for each coil are given in Table 1.

To monitor the stress evolution, both during pre-loading operations and during powering tests, strain gauges were

This work was supported by the U.S. Department of Energy, Office of Science, Office of High Energy Physics, through the US LHC Accelerator Research Program (LARP) and by the High Luminosity LHC project at CERN. The U.S. Government retains and the publisher, by accepting the article for publication, acknowledges that the U.S. Government retains a non-exclusive, paid-up, irrevocable, world-wide license to publish or reproduce the published form of this manuscript, or allow others to do so, for U.S. Government purposes.

S. Stoynev, G. Chlachidze, G. Ambrosio, R. Bossert, J. DiMarco, E. Holik, S. Krave,F. Nobrega, D. Orris, T. Strauss, C. Sylvester, M. Tartaglia, G. Velev, M. Yu are with Fermi National Accelerator Laboratory, Batavia, IL 60510, USA (S. Stoynev e-mail: stoyan@fnal.gov).

M. Anerella, A. Ghosh, J. Schmalzle, P. Wanderer are with Brookhaven National Laboratory, Upton, NY 11973, USA.

D. Dietderich, A.R. Hafalia, M. Marchevsky, H. Pan, S. Prestemon, E. Ravaioli, G. Sabbi, and X. Wang are with the Lawrence Berkeley National Laboratory, Berkeley, CA 94720 USA.

E. Cavanna, P. Ferracin, P. Grosclaude, M. Guinchard, S. Izquierdo Bermudez, J.C. Perez, E. Todesco, G. Vallone are with CERN, TE Dept. CH-1211 Geneva.

H. Felice is with CEA Saclay, 91190 Saclay, France.

T. Salmi is with Tampere University of Technology, 33720 Tampere, Finland.

TABLE I
SHORT SAMPLE LIMITS AND CORRESPONDING GRADIENTS

Coil number	SSL at 4.3/1.9 K (kA)	Gradient at 4.3/1.9 K (T/m)
Coil 3	20.12/22.28	159.2/174.6
Coil 5	19.73/21.85	156.4/171.5
Coil 103	19.55/21.50	155.2/169.1
Coil 104	19.78/21.78	156.8/171.0
MAGNET	19.55/21.50	155.2/169.1

The magnet SSL is the same as the lowest SSL found in coils.

mounted in different parts of the magnet providing stress information in azimuthal and axial directions on coil-poles, shells and rods (axial only). Voltage tap signals were read-out

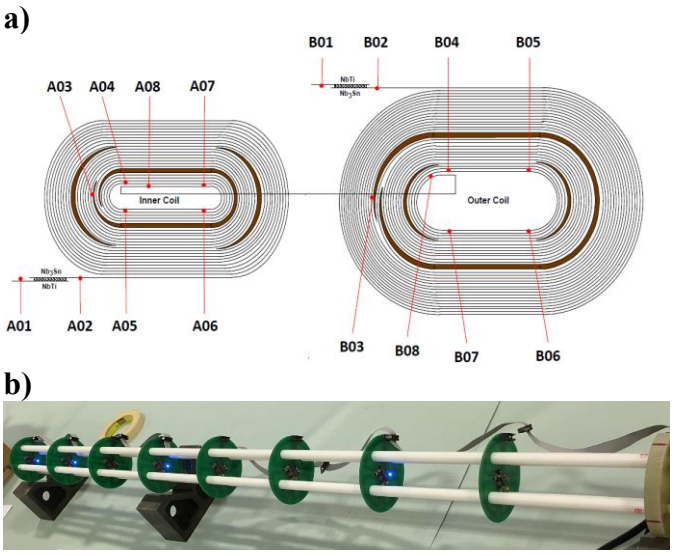

Fig. 1.(a) Voltage tap locations in the inner (left) and outer (right) coil layers; (b) Quench antenna with variable distance between sensor elements to insert in the warm bore

defining segments inside coils per the schematics on Fig. 1a. A quench antenna [8] with eight-plane stack of electromagnetic sensor couples was inserted in the warm bore for improved quench location determination, Fig. 1b. Voltage tap and quench antenna signals were both used in quench characterization and analysis.

III. MQXFS1 COMBINED TEST RESULTS

MQXFS1 went through three testing cycles with different pre-stress levels – in February-April 2016 (MQXFS1a), September-December 2016 (MQXFS1b) and May-July 2017 (MQXFS1c). The main goals of the tests included training and examination of its characteristics, magnetic measurements (see [9]) and magnet protection studies (see [10]).

A. Magnet stress monitoring

The main reason for performing several test cycles with MQXFS1 is visualized on Fig.2 where potentially harmful coil

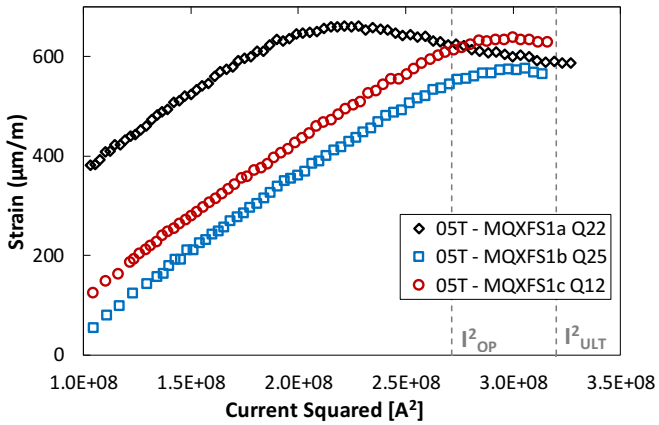

Fig. 2. Azimuthal strain ("T") measured by a gauge attached to the inner layer of coil 5. It is representative of dynamics in coils during ramp up operations. Quenches toward the "end" of training are shown (number indicated after "Q" in the legend). The peaks in the curves indicate "un-loading". As seen, in the first test cycle it was at ~15 kA, and in MQXFS1 -b and -c it shifted to ~17 kA. Operational and ultimate current levels are shown with dotted lines.

"un-loading", separation of the coil from the pole, was observed too early in current ramps. As seen, in the first test cycle it was at ~15 kA. To correct that, the azimuthal pre-stress was increased for the second test cycle. The axial pre-stress was increased for the third test cycle because of multiple training quenches in the end sections of the magnet suggested inadequate axial stress balance. The stress was monitored with a "LARP" and a "CERN" type strain gauge systems in parallel allowing a close cross-validation. The two systems had significant differences: strain gauge manufacturer, characteristics and test configurations; current source and DAQ systems; teams involved. Measurements from both were later compared to a 3D finite element analysis (FEA) estimates for the magnet and were used in mechanical validation and monitoring during the tests. Detailed mechanical analysis of the support structure and from the first MQXFS1 test were reported earlier in [11].

Whereas Fig. 2 is about stress dynamics during magnet powering, Fig. 3 gives the azimuthal stress behavior on the shell following different steps in MQXFS1b, assembly and test. Data are compared to FEA estimates. Similarly, strain gauge data from other gauges were monitored in all test cycles

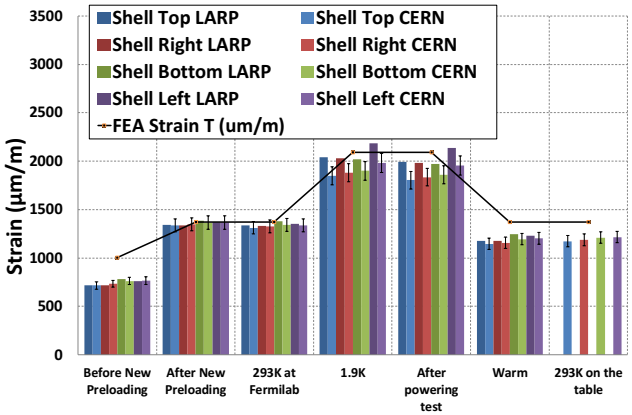

Fig. 3. Azimuthal strain on the shell in MQXFS1b in various phases. Comparisons between "LARP" and "CERN" readings on one hand and FEA calculations on the other indicate acceptable level of understanding.

of MQXFS1 with acceptable level of consistency between model expectations and observations. The few percent deviation is thought to be due to k-factor (temperature) corrections, influence of lead resistances in the signal wires and thermocouple effects. Overall the two independent stain gauge systems gave consistent results which were largely in agreement with calculations. More general mechanical analysis for short QXF magnets is found in [5], [12].

B. *Magnet Training*

In all tests quench training was performed at 1.9 K with several "control" quenches at 4.5 K to assess the quench current temperature margin. Fig. 4 presents the training summary of MQXFS1. In all cycles the magnet reached operational (I_{OP}) and ultimate (I_{ULT}) current levels. I_{ULT} is the ultimate current that these magnets may reach in LHC if it will operate above nominal energy (7 TeV), and it provides 8% margin above nominal gradient.

The MQXFS1a training proceeded with multiple quenches in all the coils. The magnet did not fully train and saw no significant detraining quenches. MQXFS1b in contrast continued with somewhat slower training with several detraining quenches observed, all in a location likely close to the transition between the end-part and the wedge in the inner layer lead-end of coil 3 – a "weak spot" (detailed analysis in [13]). Despite the increased azimuthal pre-load the magnet demonstrated good memory starting re-training just below the last quench current from the previous cycle. This confirmed the conclusions from the earlier memory test in MQXFS1a with a thermal cycle. MQXFS1c instead saw over 2 kA drop at the start of re-training and continued with slow training and detraining quenches with most of the quenches in the suspected "weak spot" in coil 3, similarly to MQXFS1b. As can be seen in Fig. 5, a detraining quench of large magnitude occurred in coil 104 as well suggesting the effect was not localized. The cause detraining could be in the axial un-loading (loss of coil pre-stress) before increasing the axial prestress. It should be noted that there was no "un-loading" when the azimuthal prestress was increased for MQXFS1b. In addition, the axial prestress may have been increased too much for a magnet that already developed some weak spots in the previous test. Overall the magnet performed well reaching 95.8% of the magnet SSL at 4.5 K and 88.4% of the magnet SSL at 1.9 K.

A different perspective of the same training data is presented on Fig. 5 – coil training. Quench numbers are arranged per their occurrence in each coil separately. CERN coils behaved somewhat similarly to the LARP coil #2 tested in a mirror configuration [14] with a steady though not constant training rate. They never reached a plateau. "LARP" coils demonstrated very fast initial training but the curve flattened with multiple detraining quenches. The stability of quench current at 4.5 K, over two test cycles with otherwise erratic training behavior, implies cable degradation at the level of 5-6%. The analysis of training quench locations revealed that coil 3 and 5

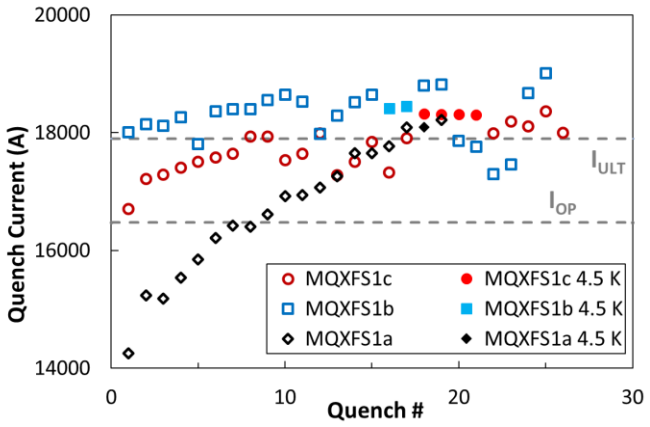

Fig. 4. Quench training current histories from the three test cycles performed with MQXFS1. I_{OP} and I_{ULT} are represented as dashed lines. The few 4.5 K quenches explicitly are shown on the plot with filled markers

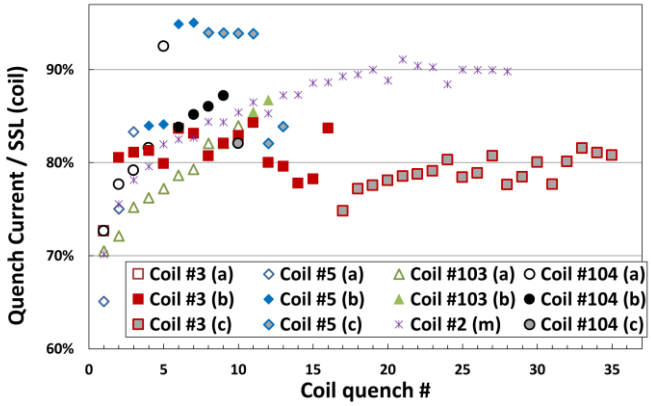

Fig. 5. Coil training in MQXFS1 (test cycles indicated after the coil numbers) and MQXFM1 (the mirror magnet, "m", with coil #2). The current is normalized to the temperature dependent SSL of each coil; no quench occurred in coil 103 in the last test cycle; all 4.5 K quenches done are clearly visible at a level of ~ 95% of SSL.

may have the same "weak spot" and large amount of quench data with repeatable matching characteristics from coil 3 supports the idea of such a "weak spot". "CERN" and "LARP" coils were developed and fabricated independently [15] and differences in wedge material ("softness" and thermal expansion) are candidates to explain some performance differences between the two types of coils.

C. *Ramp Rate Dependence*

Fig. 6 presents the ramp rate dependence of the quench current in MQXFS1. This dependence was very weak for ramp rates up to 300-350 A/s after which there was a sharp decline of the quench current. There was not such a clear border region in the mirror-magnet test due to different closure of magnetic flux lines, in particular in the mid-plane area. The quenches at the ramp rate plateau were similar in characteristics to the training quenches. Beyond that point all quenches developed in the mid-plane area, exclusively in coil 5 in the last two cycles. This behavior did not change with different pre-stress levels nor pointed to indications of cable degradation after multiple magnet tests with extended programs.

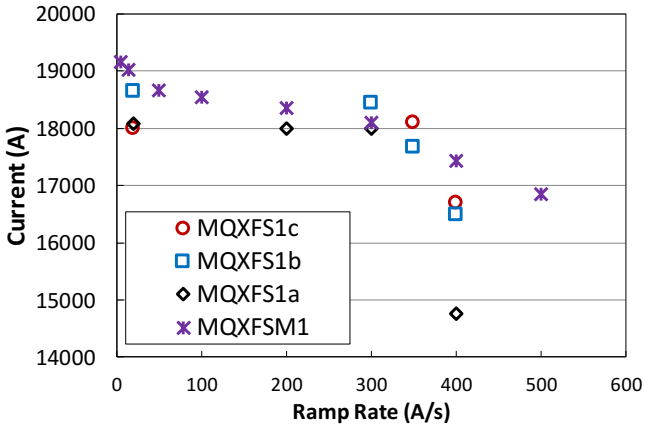

Fig. 6. Quench current ramp rate dependence in MQXFS1 and MQXFM1. It should be noted that only MQXFM1 was fully trained when quenches at different ramp rates were performed.

D. RRR and training

Higher RRR, within given limits, is associated with better conductor stability [16]. We investigated the relation between the first quench current in a coil and the measured RRR and observed an unexpected (negative) correlation, Fig. 7. Similar observations were reported for other magnet series in [17] as well. Although the correlation observed cannot lead to direct conclusions it is a factor to consider and further explore. A more general observation that low RRR coils in MQXFS1 performed better is of lesser importance as it seems apparent other magnet-specific factors contributed to that.

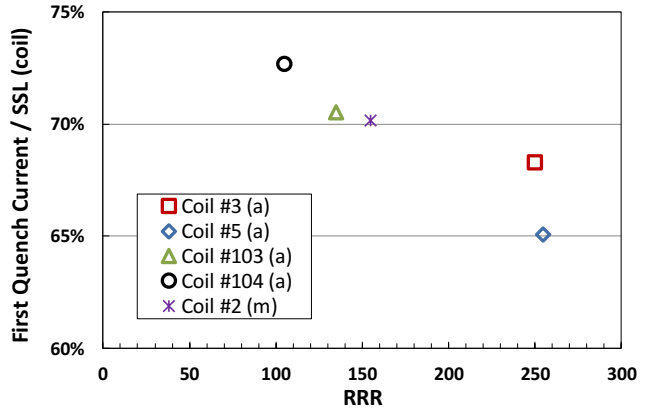

Fig. 7. Normalized to SSL first quench current vs RRR. Results are presented per coil and include coil #2 in the mirror-magnet test (denoted by "m"). MQXFS1 measurements were from the first test cycle (a).

E. Holding current tests

The magnet was ramped to ultimate current (17890 A) and the current held for two hours in MQXFS1b. In MQXFS1c there was no explicit holding current test but during magnetic measurements the current was at flat top of 16480 A for up to two hours. Those tests demonstrated the capability of the magnet for stable operation. The magnet operated at high current for eight hours during tests in MQXFS1a [4].

F. Splice resistance measurements

Splice resistance measurements were performed in all the test cycles with consistent results. Although for all Nb_3Sn-NbTi splices in the magnet Tin-Silver soldiering material was used, the splice tooling for "LARP" coils (3 and 5) did not allow for optimal heat-flow. This affected the splice quality leading to the expectation of higher resistance for "LARP" splices. Fig. 8 presents the measurement results. The splice resistances were safely below an acceptable value of 1 nΩ but "CERN" splices had consistently lower resistance.

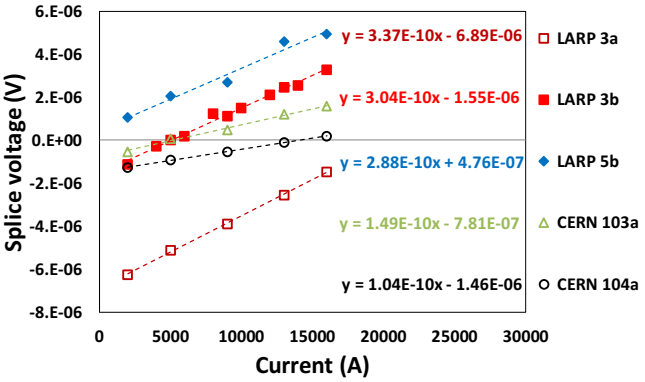

Fig. 8. Splice resistance measurements in MQXFS1. Resistance is extracted as the slope of the measured V-A dependence as given on the plot, instrumental offsets are irrelevant in the context. "LARP" and "CERN" splices correspond to coils (3,5) and (103,104), respectively; "a" and "b" denote the inner and outer layer leads, respectively. Measured resistances are between 0.10 and 0.34 nΩ with the uncertainty estimated as 0.06 nΩ.

IV. Conclusion

The first short model large aperture Nb_3Sn quadrupole MQXFS1 underwent three successful test cycles. Despite changes to pre-stress levels after the first cycle the magnet did not train faster and instead showed some detraining behavior associated almost exclusively with a single quench location in one of the coils. Nevertheless, the magnet reached 88.4% of SSL at 1.9 K and 95.8% of SSL at 4.5 K. In all cycles LHC operational and ultimate current targets were met. The magnet exhibited stable operation at currents up to the ultimate level (17890 A) for extended periods of time. The magnet demonstrated good training memory though temporal prestress release before the third cycle was the likely cause of some initial detraining. No changes in quench current ramp rate dependence was observed between test cycles at high ramp rates.

RRR measurements showed (negative) correlation with the first quench current in coils. Splice resistances in MQXFS1 were well below acceptable limits.

Acknowledgment

The authors thank the technical staff at BNL, LBNL, FNAL and CERN for contributions to magnet fabrication and test.

REFERENCES

[1] G. Sabbi, "Nb3Sn IR quadrupoles for the high luminosity LHC," *IEEE Trans. Appl. Supercond., vol. 23, no. 3, Jun. 2013, Art. no. 4000707.*

[2] P. Ferracin et al., "Development of MQXF, the Nb3Sn Low-β Quadrupole for the HiLumi LHC," *IEEE Trans App. Supercond. Vol. 26, no. 4, Jun. 2016, Art. No. 4000207.*

[3] G. Ambrosio, et al., "Test of the first MQXFA prototype by LARP and status of the US High Luminosity LHC Accelerator Upgrade Project preparation," *IEEE Trans. Appl. Supercond., MT25, Wed-Af-Or23,* submitted for publication.

[4] G. Chlachidze, et al., "Performance of the first short model 150 mm aperture Nb3Sn Quadrupole MQXFS for the High-Luminosity LHC upgrade," *IEEE Trans. Appl. Supercond., vol. 27, no. 4, Jun. 2017, Art. no. 4000205.*

[5] G. Vallone, et al., "Mechanical Analysis of Short Model Magnets for the Nb3Sn Low-Beta Quadrupole MQXF," *IEEE Trans. Appl. Supercond., MT25, Mon-Mo-Or3-07,* submitted for publication.

[6] G. Ambrosio, et al., "MQXFS1 Quadrupole Design Report," *FERMILAB-TM-2613-TD*, Fermilab 2016.

[7] G. Ambrosio, et al., "MQXFS1 Quadrupole Fabrication Report," *FERMILAB-TM-2660-TD*, Fermilab 2017.

[8] M. Marchevsky, et al., "Magnetic Quench Antenna for MQXF Quadrupoles," *IEEE Trans. Appl. Supercond., vol. 27, no. 4, Jun. 2017, Art. no. 9000505.*

[9] S. I. Bermudez, et al., "Geometric field errors of Short Models for MQXF, the Nb3Sn low-beta Quadrupole for the High Luminosity LHC," *IEEE Trans. Appl. Supercond., MT25, Wed-Af-Or23-04,* submitted for publication.

[10] E. Ravaioli, et al., "Performance of the quench protection system of the first LARP-CERN quadrupole magnet models," *IEEE Trans. Appl. Supercond., MT25, Wed-Af-Or24-01,* submitted for publication.

[11] M. Juchno, et al., "Mechanical Qualification of the Support Structure for MQXF, the Nb3 Sn Low-β Quadrupole for the High Luminosity LHC," *IEEE Trans. Appl. Supercond., vol. 26, no. 4, Jun. 2016, Art. no. 4005506.*

[12] G. Vallone, et al., "Mechanical Performance of Short Models for MQXF, the Nb3Sn Low-β Quadrupole for the Hi-Lumi LHC," *IEEE Trans. Appl. Supercond., vol. 27, no. 4, Jun. 2017, Art. no. 4002906.*

[13] G. Ambrosio, et al., "Quench Location in the LARP MQXFS1 prototype," *IEEE Trans. Appl. Supercond., MT25, Mon-Af-Po1.01-04*, submitted for publication.

[14] G. Chlachidze et al., "LARP MQXFSM1 (mirror) magnet test summary", *FERMILAB-TD-15-018*, Fermilab, 2015.

[15] E. F. Holik, et al., "Fabrication and Analysis of 150-mm-Aperture Nb3Sn MQXF Coils," *IEEE Trans. Appl. Supercond., vol. 26, no. 4, Jun. 2016, Art. no. 4000907*.

[16] B. Bordini, et al., "Impact of the Residual Resistivity Ratio on the Stability of Nb3Sn Magnets," *IEEE Trans. Appl. Supercond., vol. 22, no. 3, Jun. 2012, Art. no. 4705804.*

[17] S. Stoynev, K. Riemer, and A. Zlobin, "Quench Training Analysis of Nb3Sn Accelerator Magnets," *IEEE NAPAC2016 proceedings, MOPOB40, January 2017.*